Constraints on mantle flow models from geophysical data

Ondřej Čadek

Department of Geophysics, Faculty of Mathematics and Physics, Charles University in Prague

This work has been done in close cooperation with **Luce Fleitout**,
Ecole normale supérieure, Paris, France.

Special thanks to **E. Kaminski** for providing his code DRex,
and to **G. Marquart** and **H. Schmeling** for discussions on seismic anisotropy.

I am grateful to all the researchers who have made their results available through internet
(**T. Becker** and **L. Boschi**, **E. Debayle**, **S. Panasyuk**, ...).

Outline:

- **Constraining mantle flow models from geophysical data.**
  Basic concept, equations and boundary conditions. Available data.
- **Inferences of viscosity from the geoid.**
  Brief history, current state-of-art and limitations.
- **Further constraints: Dynamic topography and seismic anisotropy.**
  Theory and observations.
- **Towards more realistic mantle flow models.**
  Including plate motion, lateral viscosity variations and partial layering.
- **Synthetic inversion** of geoid, topography and seismic anisotropy data.
- **Conclusions**

• **Constraining mantle flow models**

Two strategies:

1. Solving equations of thermal convection including parameters and physical relationships estimated from mineral physics	$\Rightarrow$	Forward modeling: investigating behavior of a given physical system
2. Using geophysical data obtained at the surface or outside the Earth	$\Rightarrow$	Inverse modeling: determining the most probable values of parameters in PDEs governing mantle flow

- **Equations governing flow in the mantle**

$$
\begin{aligned}
\nabla.\boldsymbol{\sigma} + \rho\mathbf{g} &= 0 \\
\nabla.\mathbf{v} &= 0 \\
\boldsymbol{\sigma} &= -p\mathbf{I} + \eta[\nabla\mathbf{v} + (\nabla\mathbf{v})^{\tau}] \\
\mathrm{BC}(\boldsymbol{\sigma}, \mathbf{v}) &\ \ \text{at the surface and CMB}
\end{aligned}
$$

$$
\begin{aligned}
\rho C_p \frac{\partial T}{\partial t} &= -\rho C_p(\mathbf{v}.\nabla T) + \nabla.(k\nabla T) + ... \\
\rho &= \rho_0[1 - \alpha(T - T_0)] \\
\mathrm{BC}(T) &\ \ \text{at the surface and CMB}
\end{aligned}
$$

$$\begin{aligned}
\nabla.\boldsymbol{\sigma} + \rho\mathbf{g} &= 0 \\
\nabla.\mathbf{v} &= 0 \\
\boldsymbol{\sigma} &= -p\mathbf{I} + \eta[\nabla\mathbf{v} + (\nabla\mathbf{v})^{\tau}] \\
\mathrm{BC}(\boldsymbol{\sigma}, \mathbf{v}) &\ \text{at the surface and CMB}
\end{aligned}$$

+ no time evolution
+ any code (spectral, finite-element,...) can be used
+ body force can be estimated from seismic tomography ($\rho \sim V$)

− 3d spherical geometry
− variations of pressure must be evaluated at all density interfaces
− selfgravitation: $\mathbf{g} = \mathbf{g}(\rho, \boldsymbol{\sigma})$

Inferences of viscosity from the geoid: Basic concept

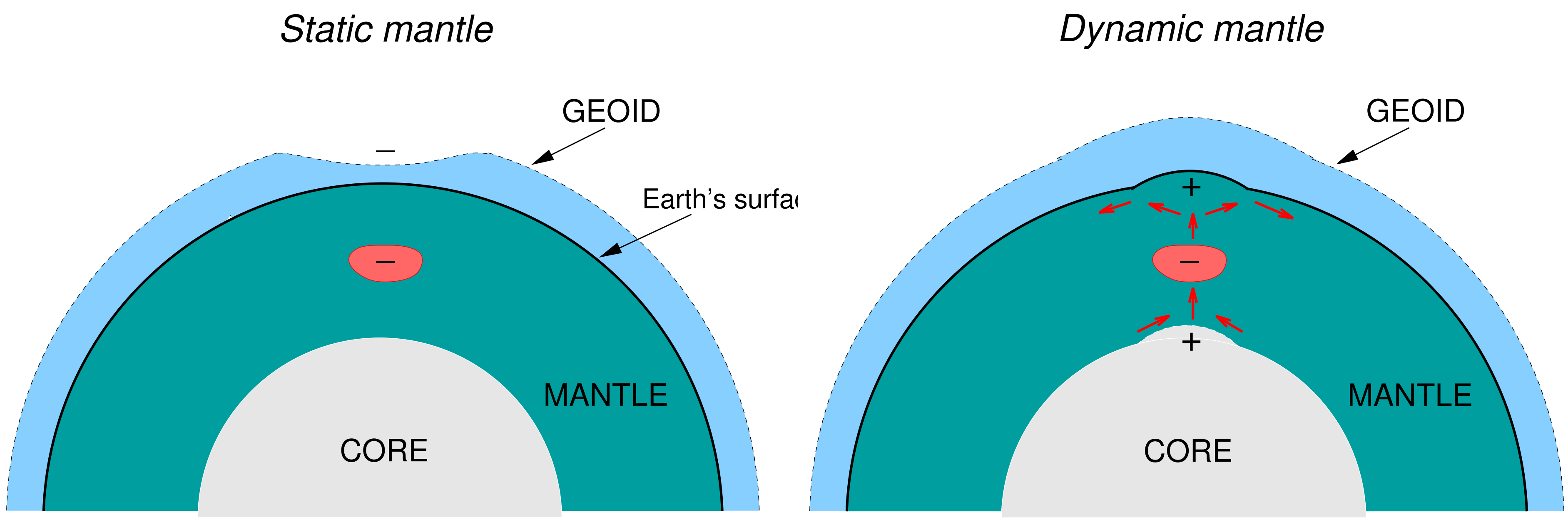

Response functions

Case 1: Isoviscous mantle

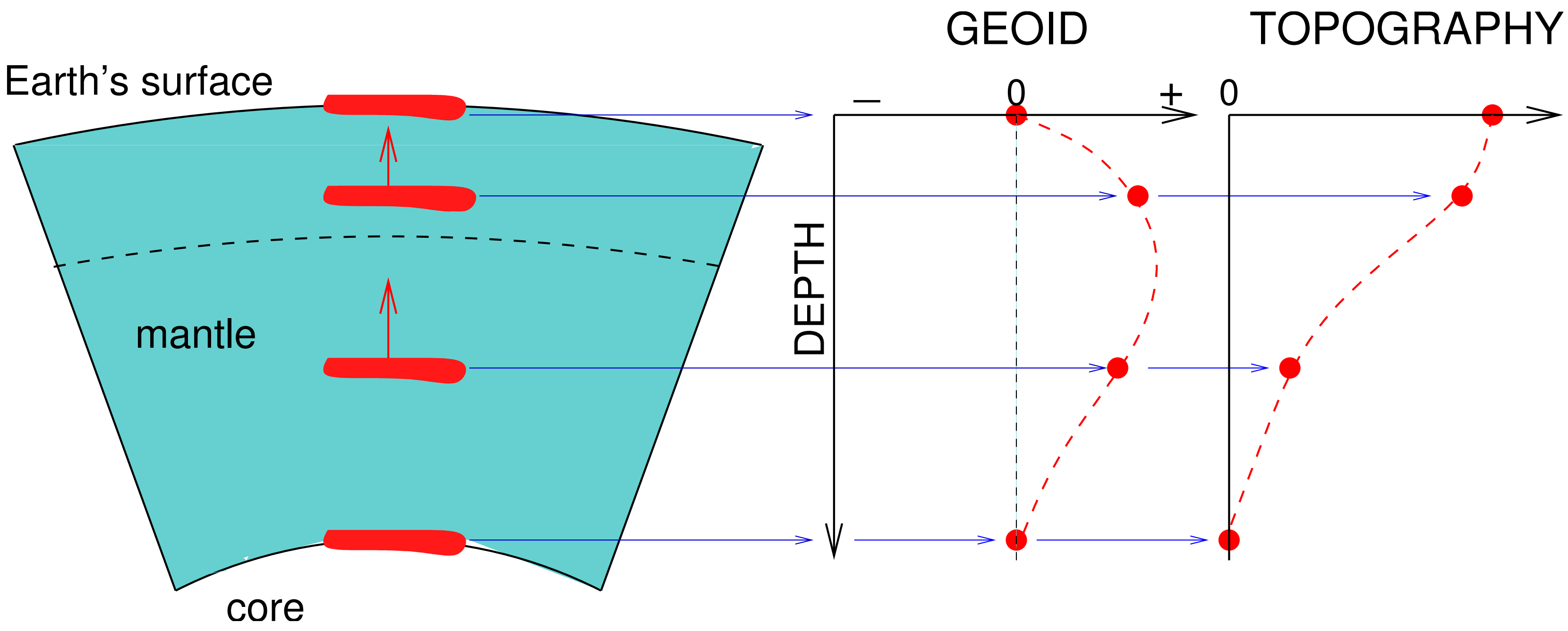

Response functions

Case 2: Viscosity increase in the lower mantle

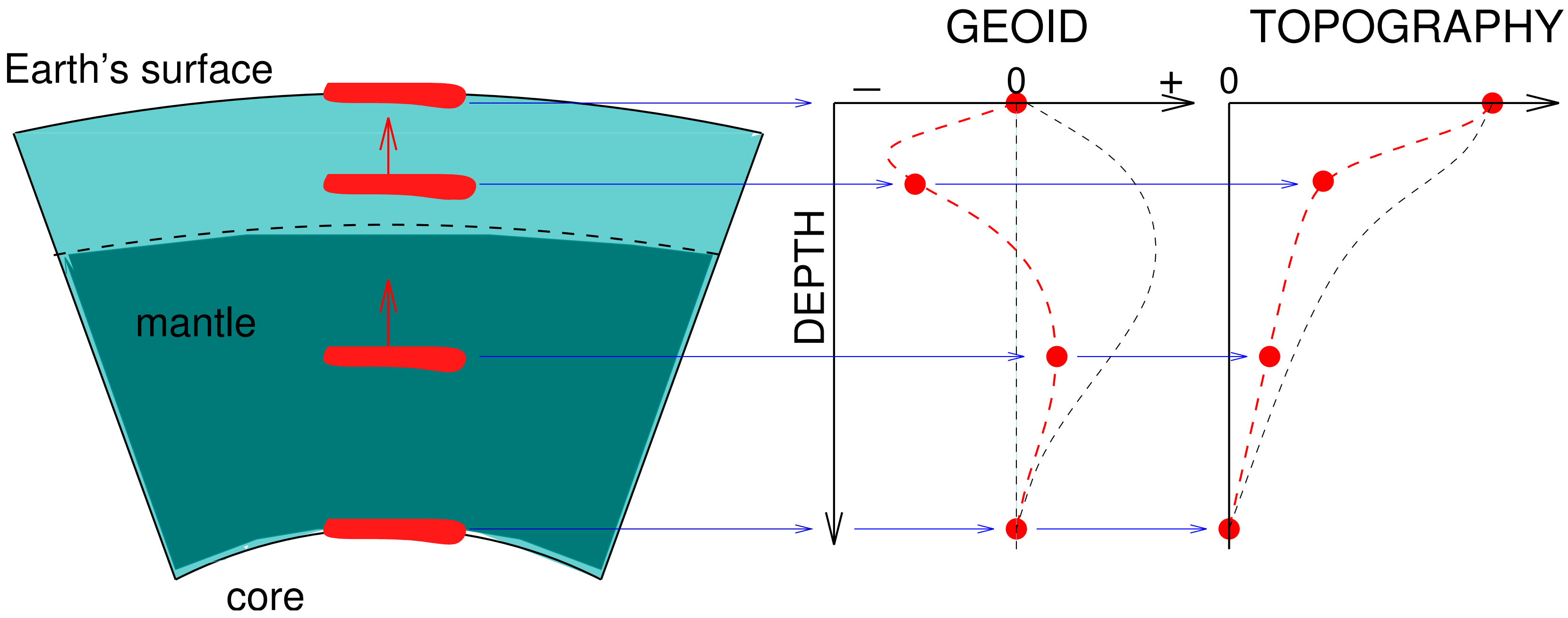

'Inferences of viscosity from the geoid': Brief history

- 1930s: Pekeris formulates the **basic idea**
- 1960s: **Theory** is developed and used by Runcorn
- 1980s: Structure information obtained from seismic tomography enables **first inversions for viscosity.**
- 1984: *Ricard et al.* and *Richards and Hager* demonstrate that the observed long-wavelength non-hydrostatic geoid is consistent with a viscosity increase with depth by a factor of $\sim$30.
- 1993: Density structure obtained from subduction history is used instead of seismic tomography data (*Ricard et al.*).

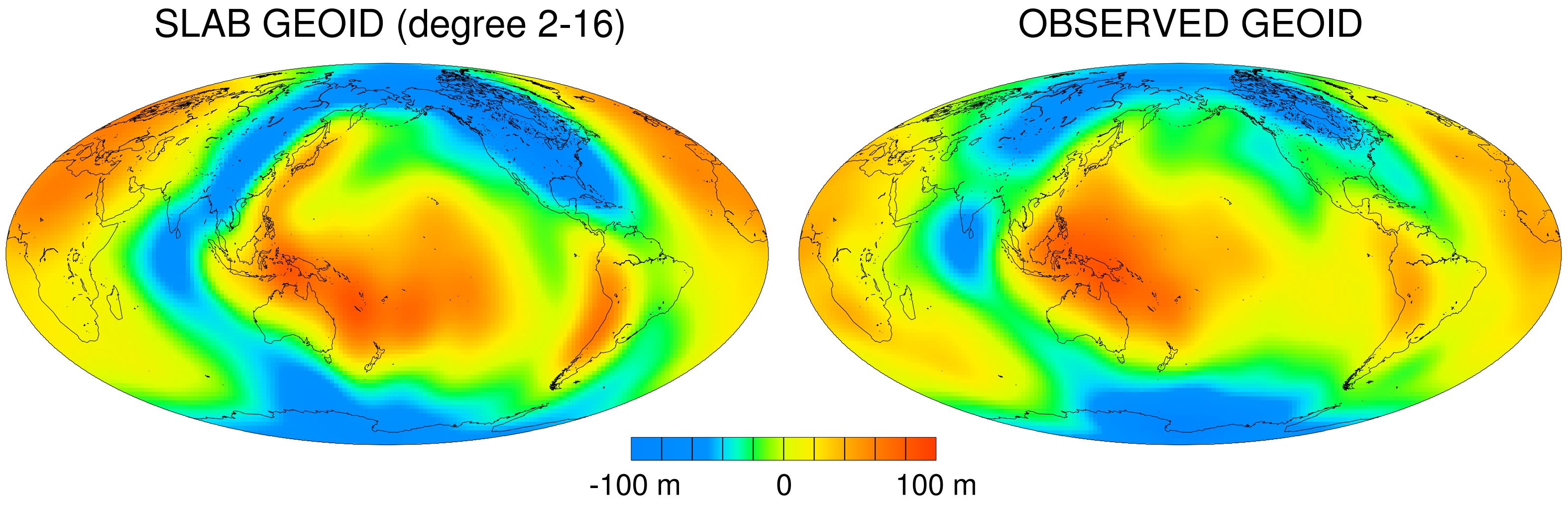

Relative viscosities: upper mantle 1, lithosphere 7, lower mantle 30.

- Since 1990: Attempts to incorporate **more constraints** (plate motion, dynamic topography, etc.) and a more **realistic rheology**
- **Free-air gravity** used as a constraint instead of the geoid (*Peltier et al.*, 1992).

Geoid:

$$h = \sum_{\ell=2}^{\ell_{max}} \sum_{m=-\ell}^{\ell} h_{\ell m} Y_{\ell m}$$

Free-air gravity:

$$f = (g/R) \sum_{\ell=2}^{\ell_{max}} \sum_{m=-\ell}^{\ell} (\ell - 1) h_{\ell m} Y_{\ell m}$$

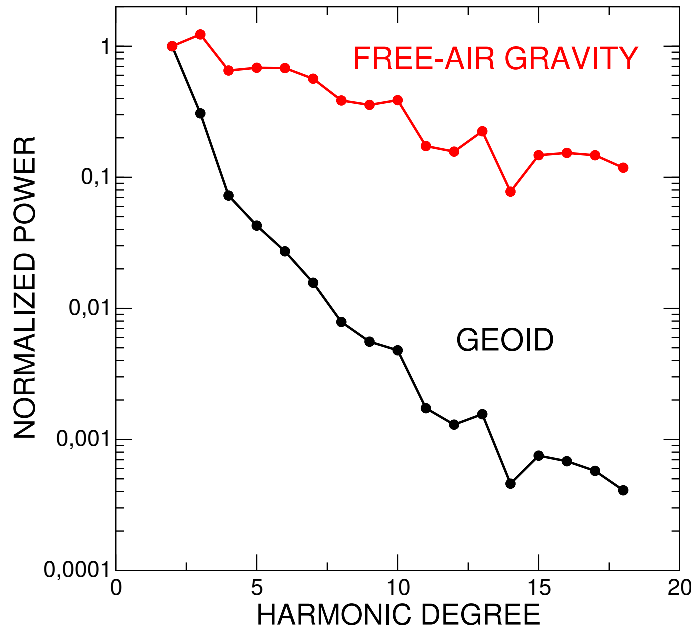

- Strong **non-uniqueness** of the inversion demonstrated (e.g. *King*, 1995).
- Attempts to include **partial layering** (*Thoraval et al.*, 1995; *LeStunff and Ricard*, 1997).

Problems:

- Whole-mantle flow models with free-slip upper boundary explain the geoid significantly better than more realistic models in which the observed **plate motion** is imposed.
- The best-fitting models are usually characterized by the lithosphere which is weaker than the lower mantle and by the absence of a pronounced asthenosphere.
- Whole-mantle flow models predict a correct geoid but usually too big amplitudes of the large-scale dynamic topography $\Rightarrow$ importance of **partial layering**.
- Role of **lateral viscosity variations**?
- Inversion of the geoid for viscosity is non-unique: **further constraints** needed.

Dynamic topography: Basic concept

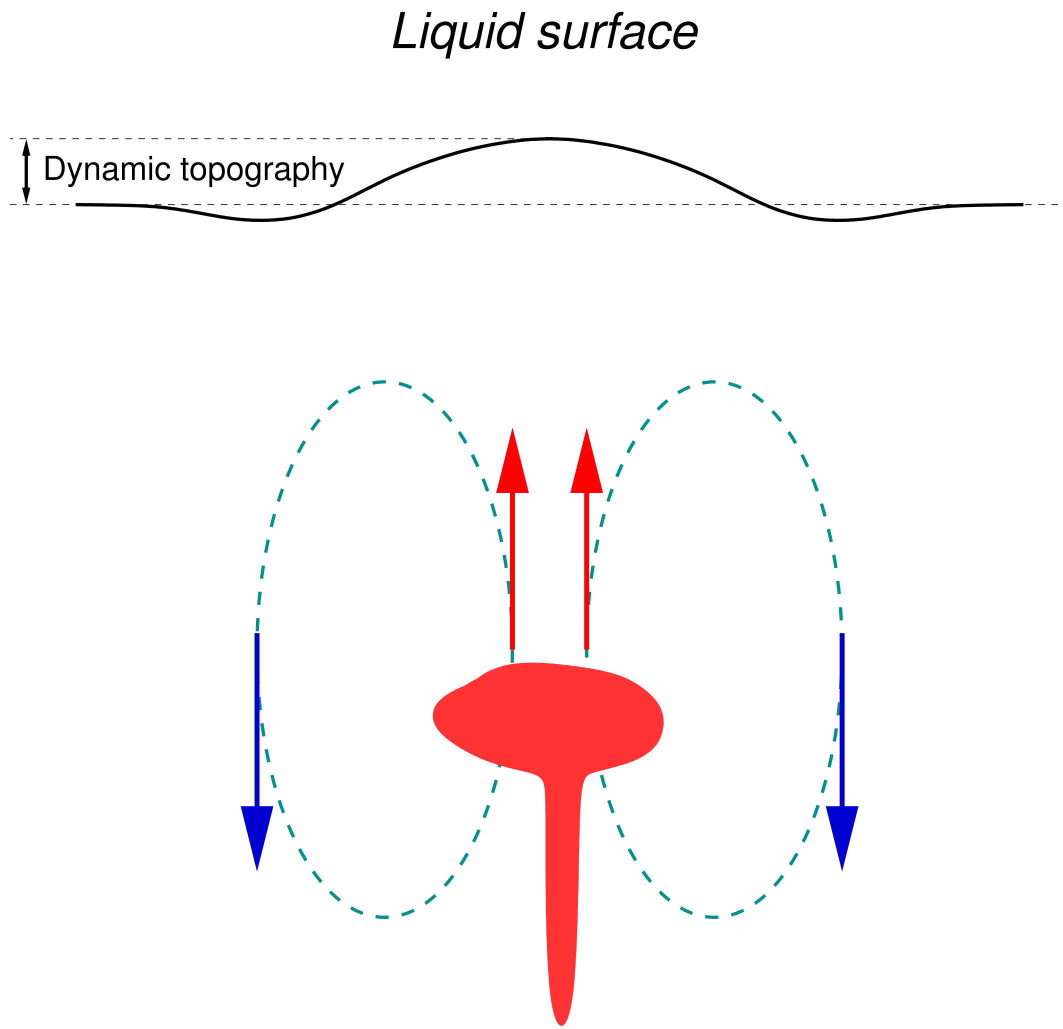

Free-slip boundary condition

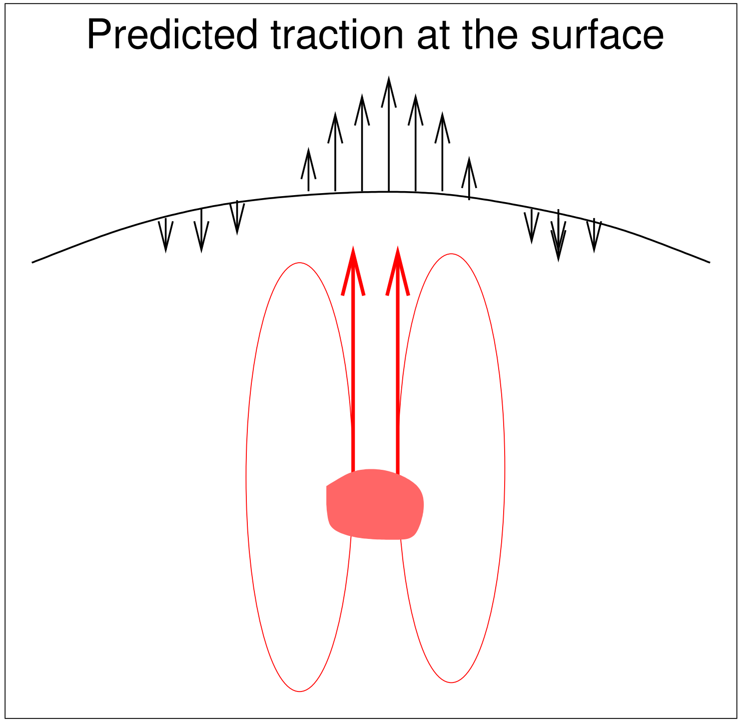

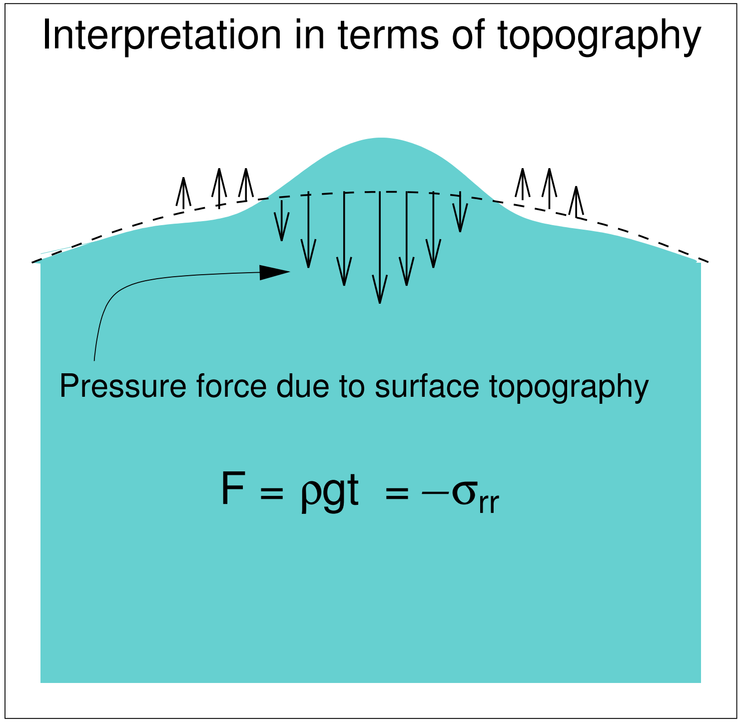

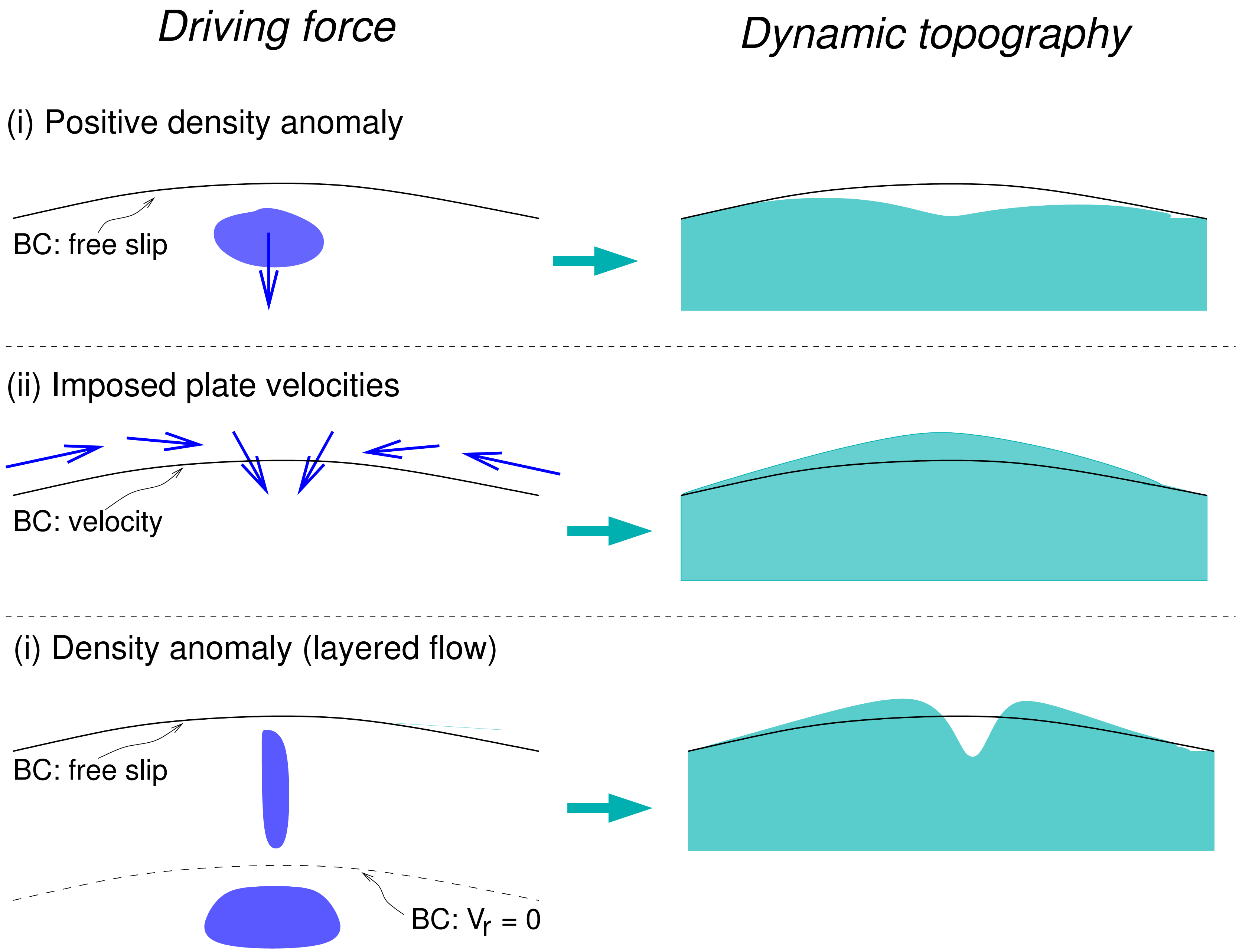

Driving force
Dynamic topography
(i) Positive density anomaly
BC: free slip
(ii) Imposed plate velocities
BC: velocity
(i) Density anomaly (layered flow)
BC: free slip
BC: V_r = 0

Dynamic topography: Observation

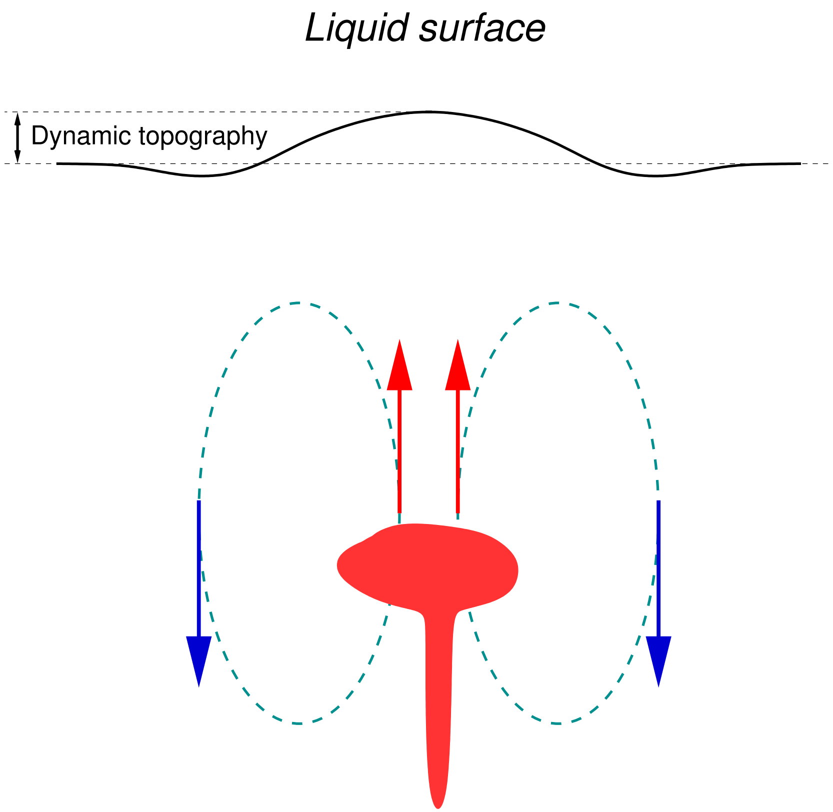

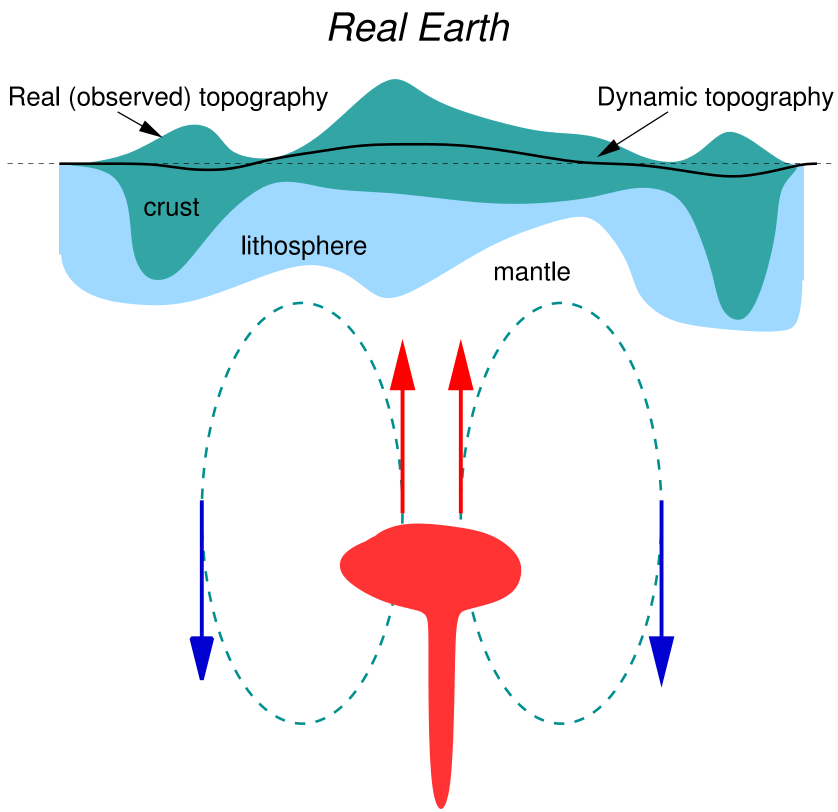

Determining dynamic topography in continental regions requires very good knowledge of lithospheric density.

1%-error in density produces 1-km error in amplitude of dynamic topography!

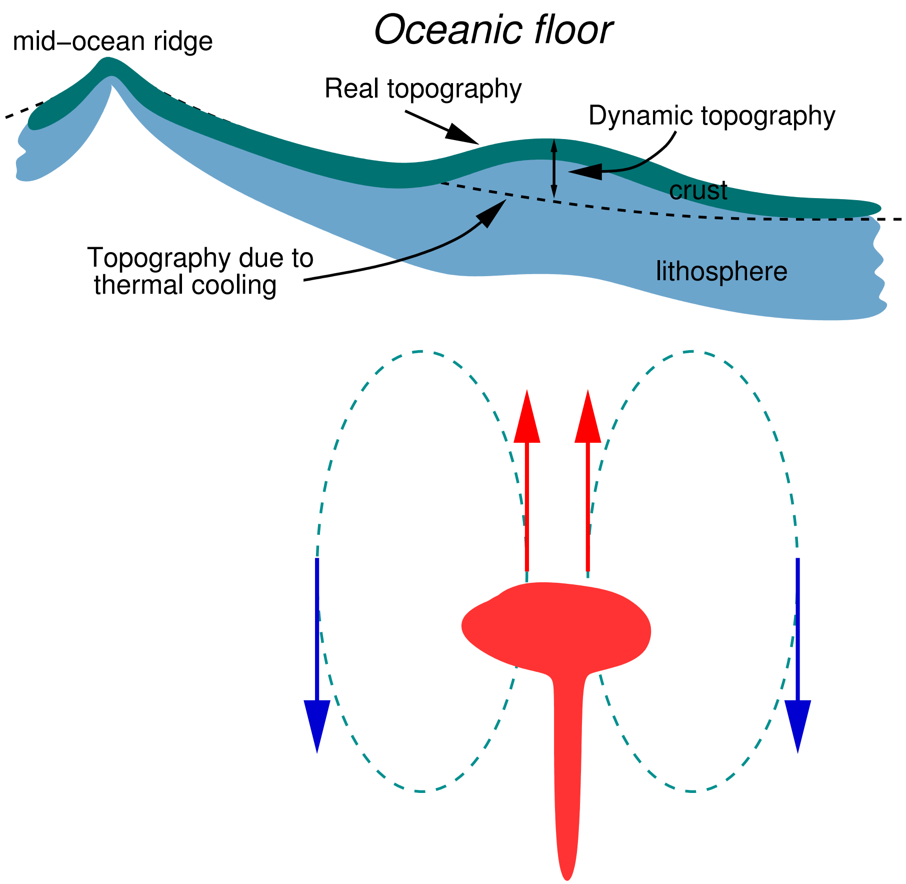
Oceanic floor
mid–ocean ridge
Real topography
Dynamic topography
crust
Topography due to
thermal cooling
lithosphere

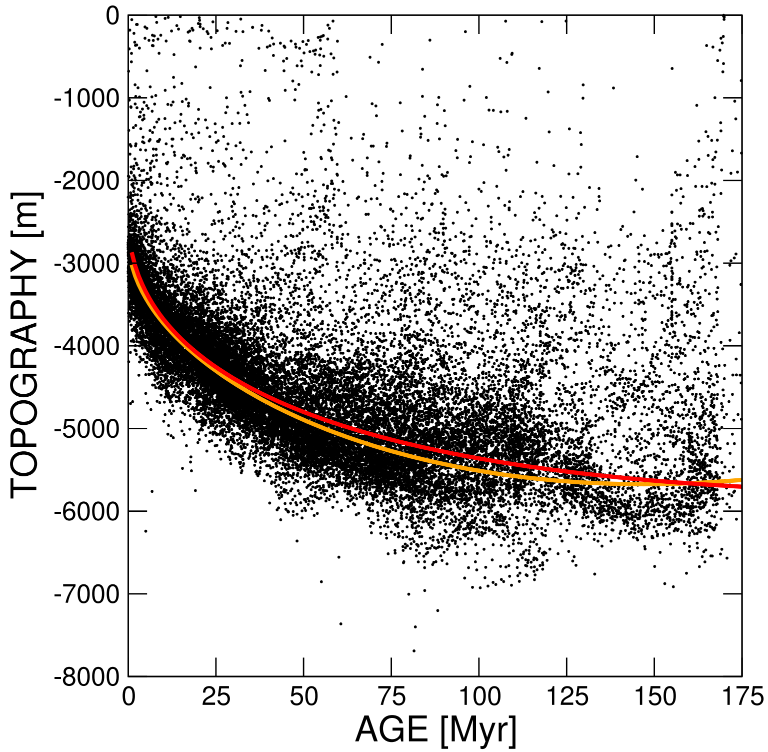
TOPOGRAPHY [m]
0
-1000
-2000
-3000
-4000
-5000
-6000
-7000
-8000
0
25
50
75
100
125
150
175
AGE [Myr]

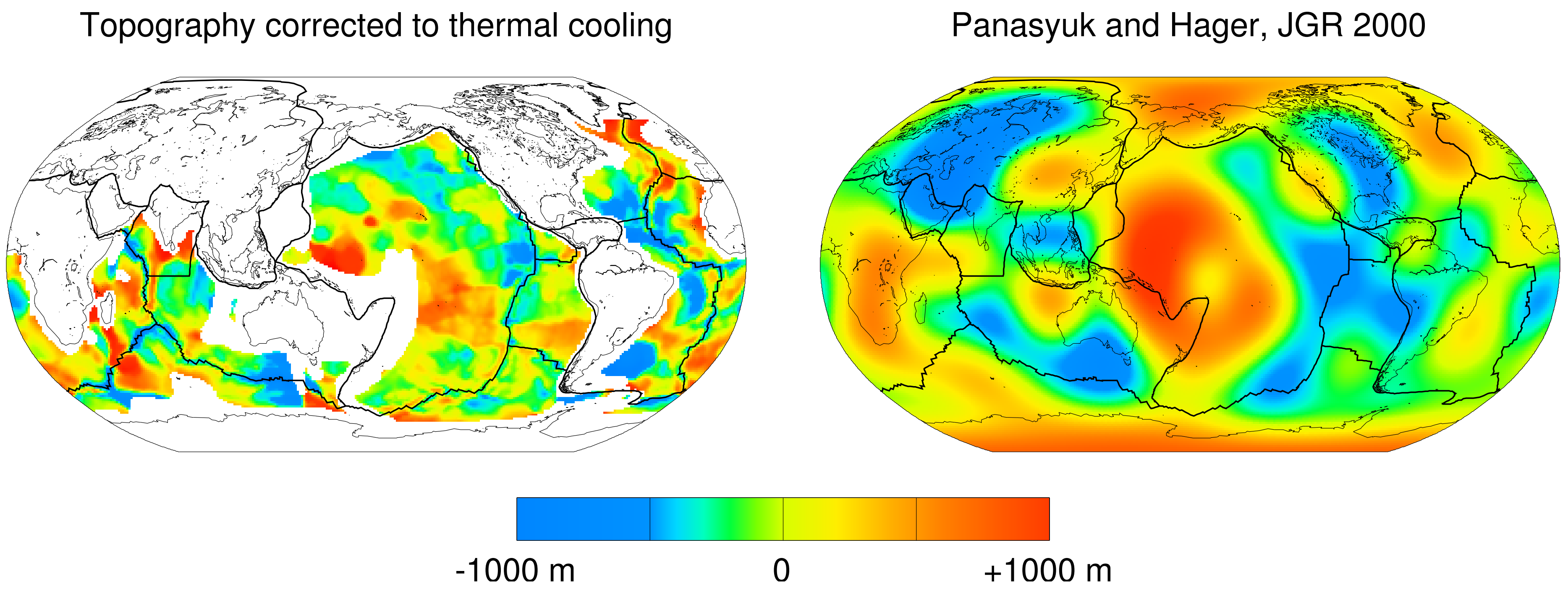

- amplitudes of the long-wavelength dynamic topography are probably smaller than 500 m (but depends on the density of continental lithosphere)
- there is no indication that the dynamic topography is positively correlated with the divergence of plate motion

Seismic anisotropy: Theory

Anisotropy can be predicted by integrating $\nabla \mathbf{v}$ along a pathline. Theory for olivine and enstatite, including recrystalization, has recently been developed by *Kaminski et al.* (program DRex, GJI 2004).

Problems:

- anisotropy is produced by dislocation creep $\Rightarrow$ non-Newtonian rheology
- computation of anisotropy requires integration of $\nabla \mathbf{v}$ in time
- how long time interval should be used for integration?
- predicted anisotropy is usually larger than the observed one
- importance of small-scale convection and composite rheology?
- computation of anisotropy is time-consuming and requires high accuracy

Seismic anisotropy: Observations

Global model of Debayle, Kennett and Priestly, Nature 2005

Depth 100 km

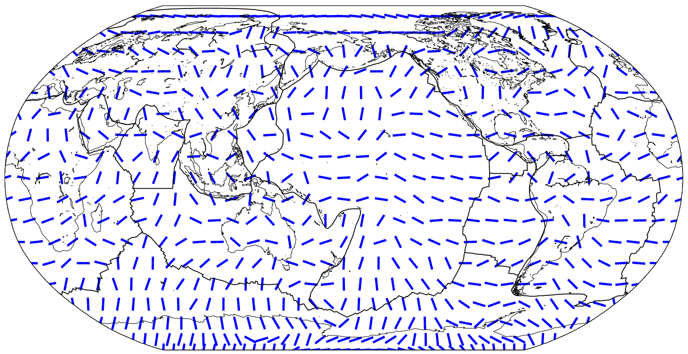

Depth 150 km

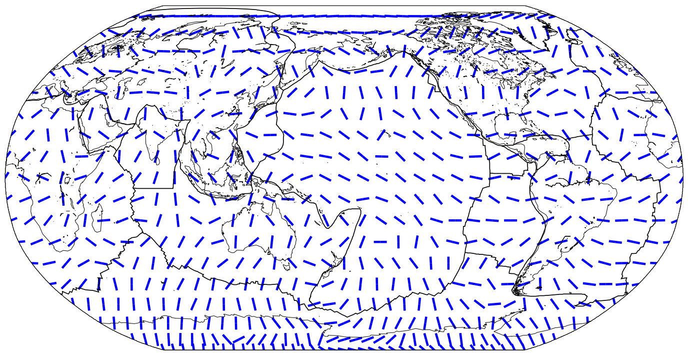

Depth 200 km

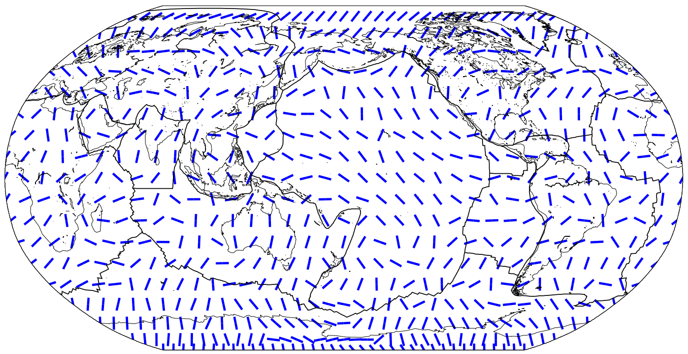

Depth 300 km

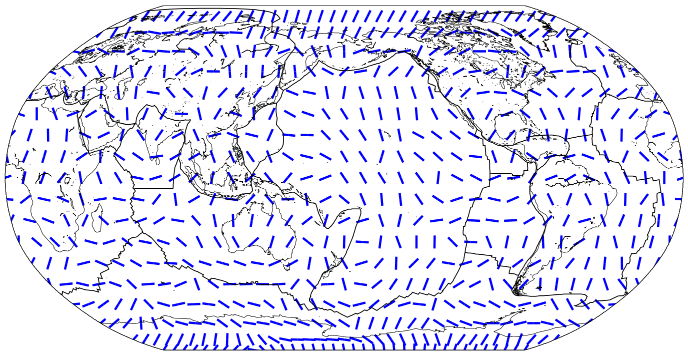

- large differences between different seismic anisotropy models
- recently, information on anisotropy in the asthenosphere has also been obtained from magnetotelluric measurements

Towards more realistic models

Solving the inverse problem for viscosity including:

- **partial layering**
- **observed plate motion**
- **known structure of lateral viscosity variations in the top 300 km (continental roots)**
- **more constraints (geoid, topography, seismic anisotropy)**

For preliminary results, see also
Čadek and Fleitout, JGR 1999, and *Čadek and Fleitout*, GJI 2003.

I. Partial layering

'Layering coefficient' λ, $0 \leq \lambda \leq 1$: $\quad S^{PL} = (1-\lambda)S^{WM} + \lambda S^{L}$

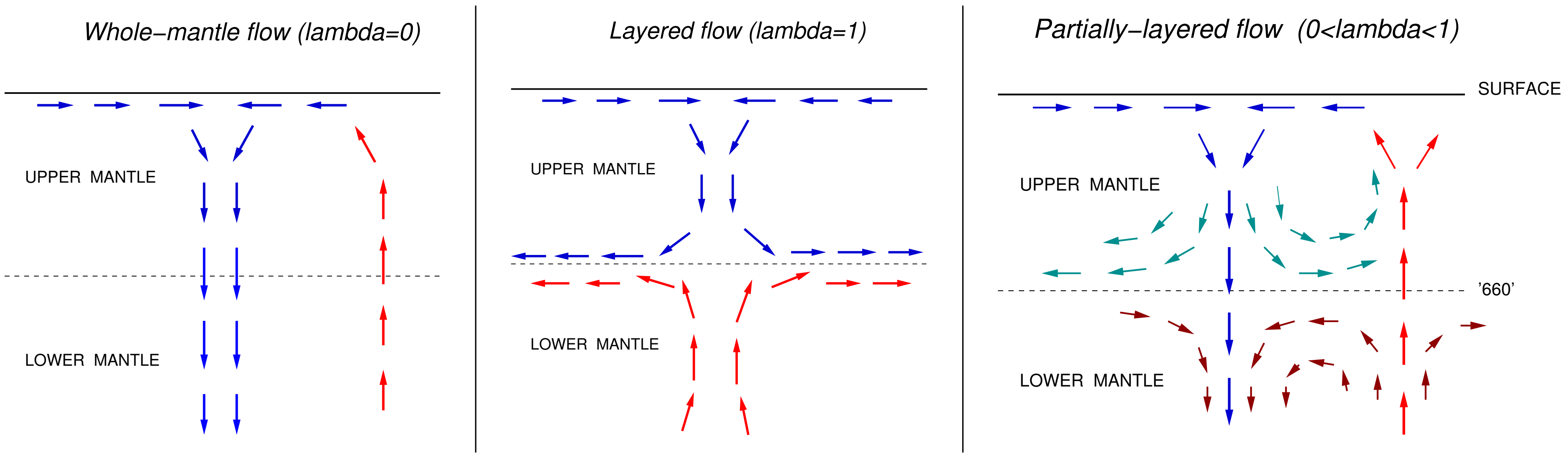

Radial component of velocity at 660 km: $V_r^{PL} = (1-\lambda)V_r^{WM}$

II. BC: Observed plate velocity prescribed at the base of lithosphere

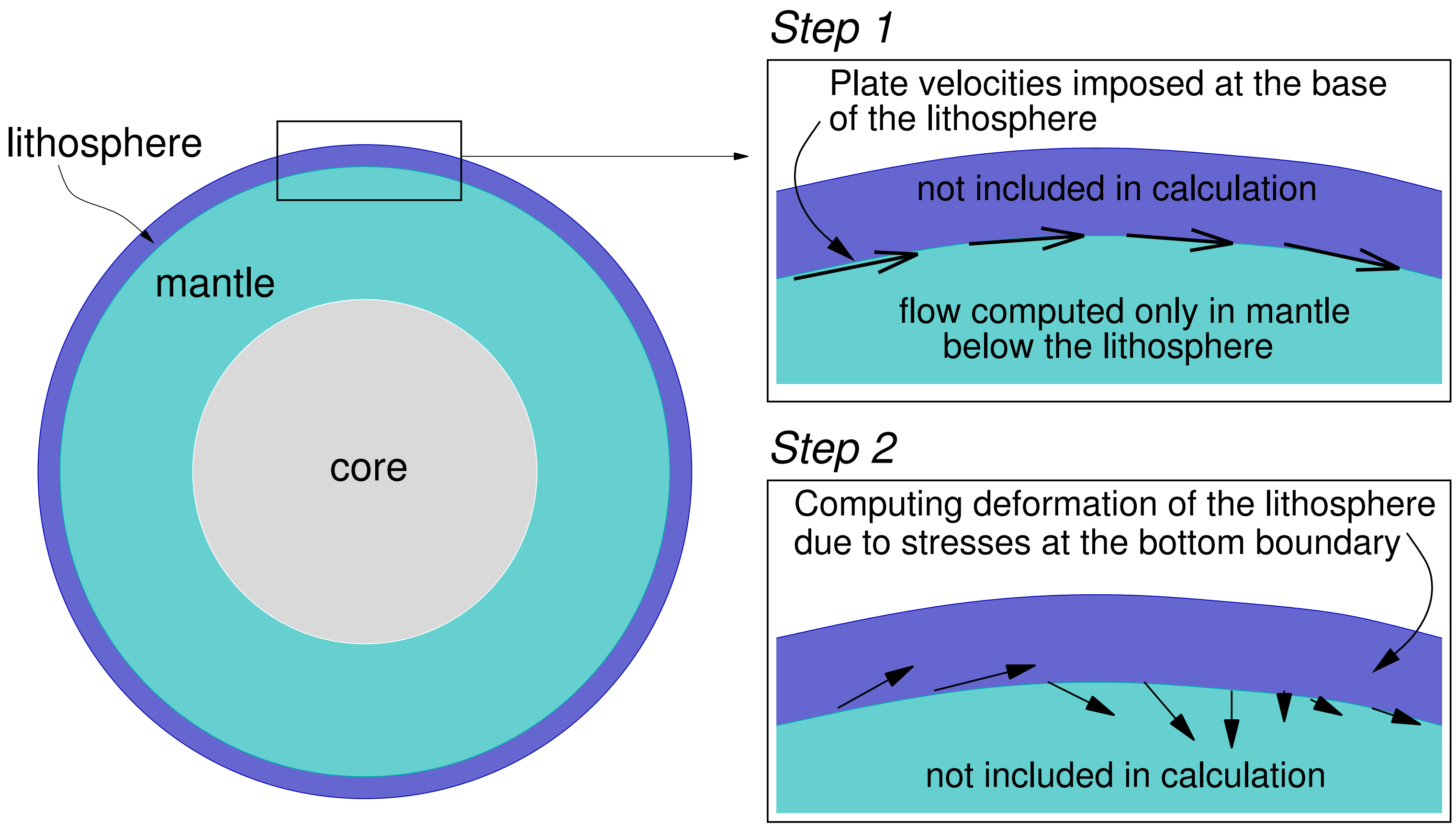

III. Lateral viscosity variations

Shields & cratons (SC)

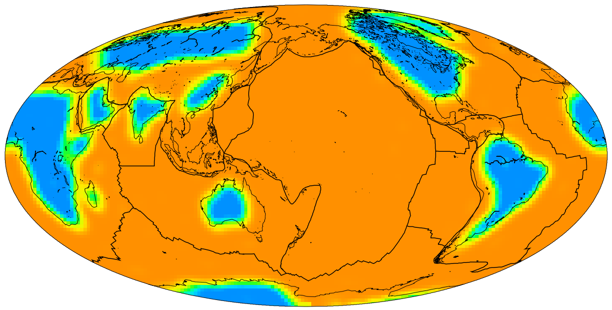

Continents I

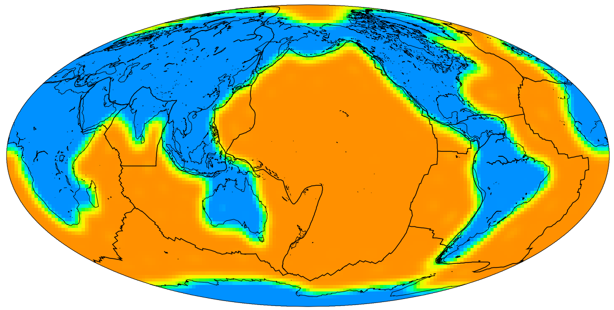

Continents II

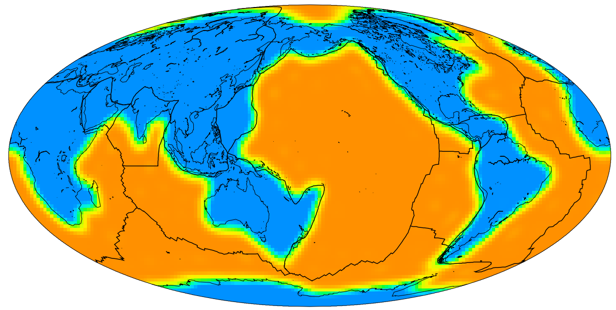

SC+oceans

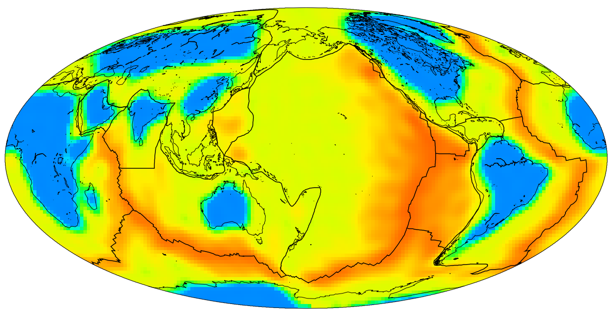

SC+oceans+slabs

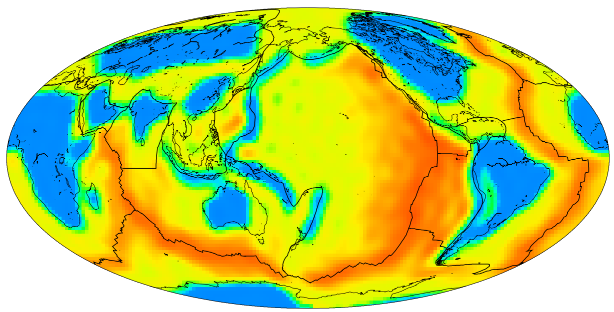

Debayle et al. (2005)

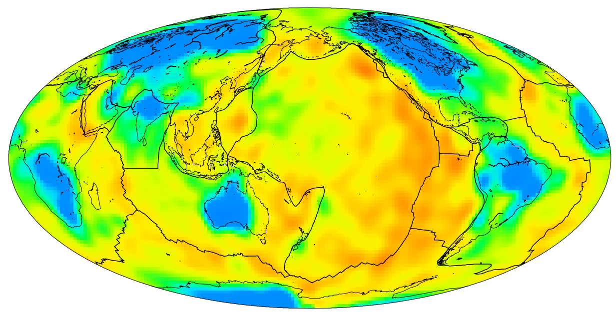

Model parameters, input data and constraints

- **Parameterization** chosen as simple as possible:

	model parameter	range explored
1	upper-mantle viscosity	$10^{19} - 10^{21}$ Pa s
2	lower-mantle viscosity	$10^{19} - 10^{24}$ Pa s
3	scaling factor for lateral viscosity variations (lateral viscosity contrast)	$1 - 100$
4	layering coefficient λ	$0.0 - 1.0$
5	velocity-to-density scaling in the upper mantle	$0.0 - 0.4$
6	velocity-to-density scaling in the lower mantle	$0.0 - 0.6$

- **Density structure**: based on differents tomographic models from the database of T. Becker and L. Boschi
- **Data constraints**: geoid and free-air gravity (degree 2-8), dynamic topography (degree 1-8) and seismic anisotropy at 150-km depth.
- **Inversion**: solved by systematic exploration of the model space

Fitting the geoid and free-air gravity

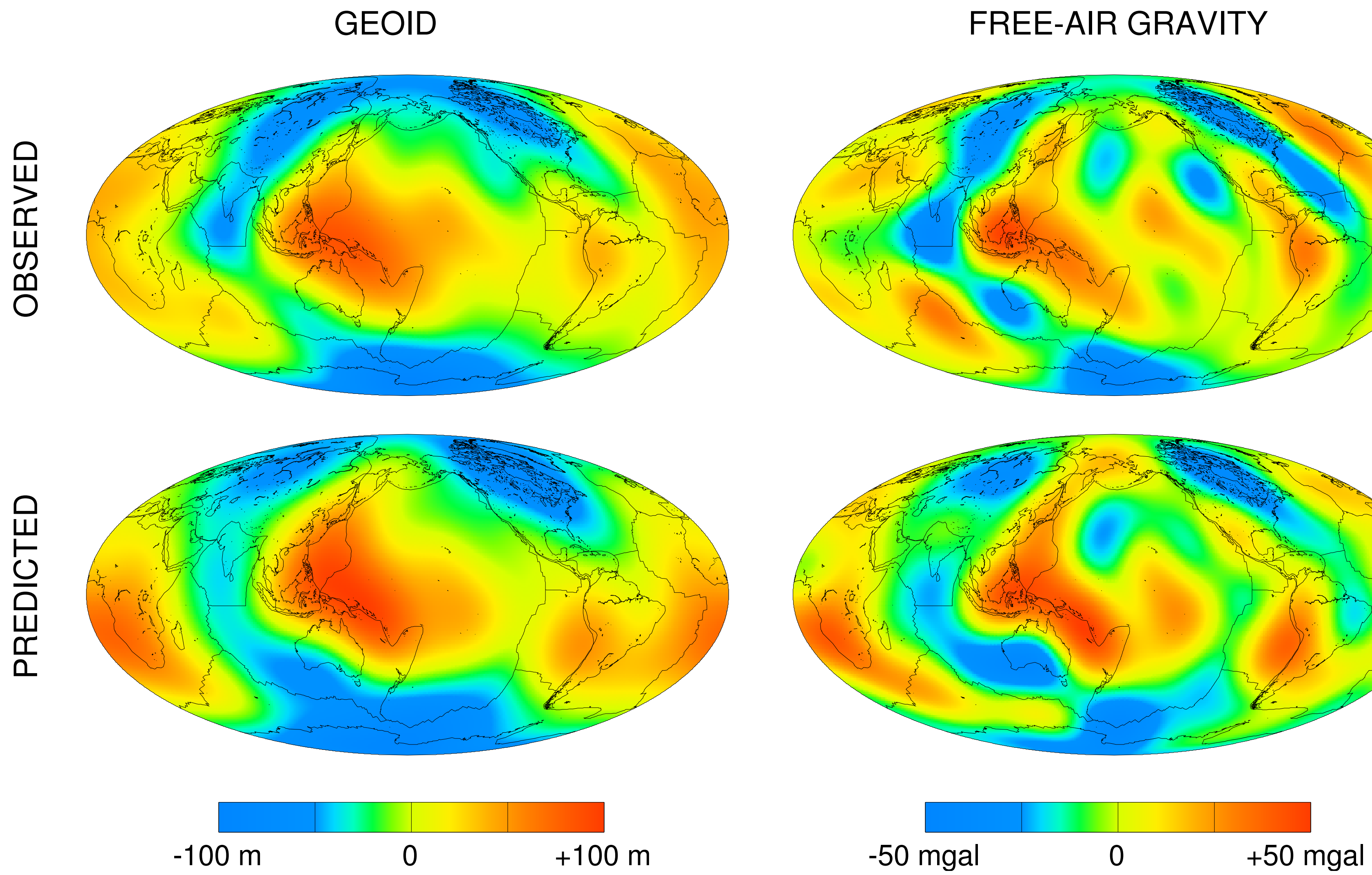

Predicted gravity [%]

LVV: Stable continents (SC)

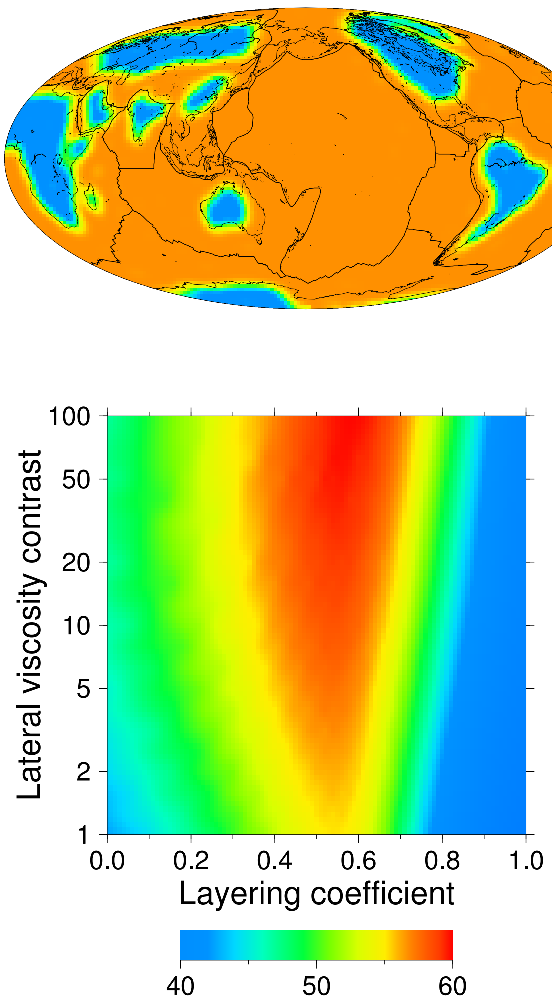

SC+slabs+young oceans

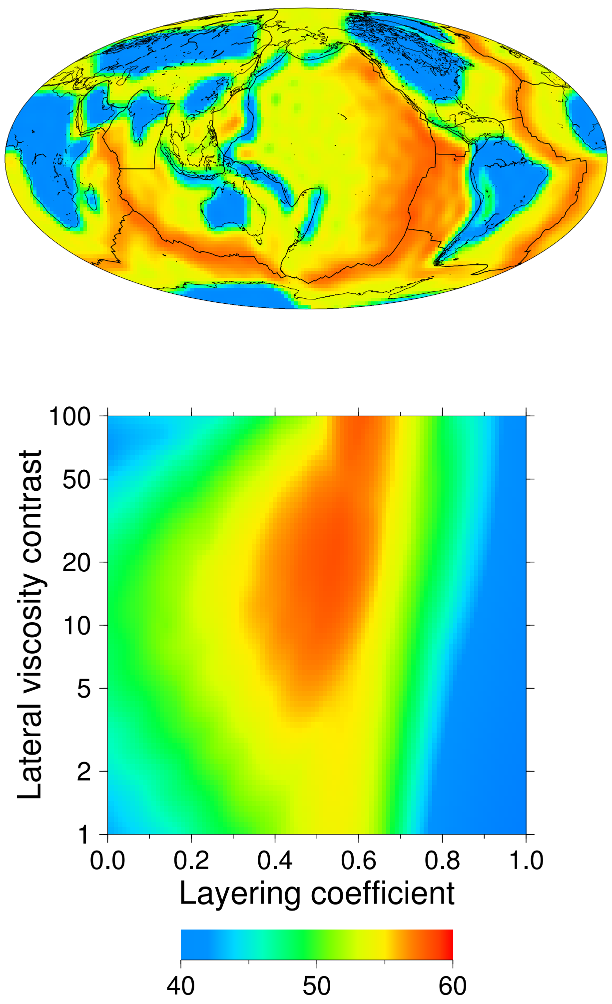

Predicted gravity [%]

LVV: Stable continents (SC)

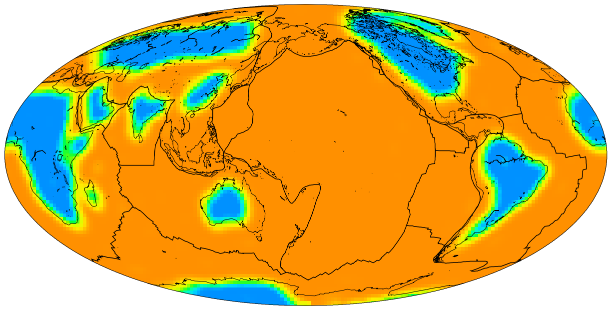

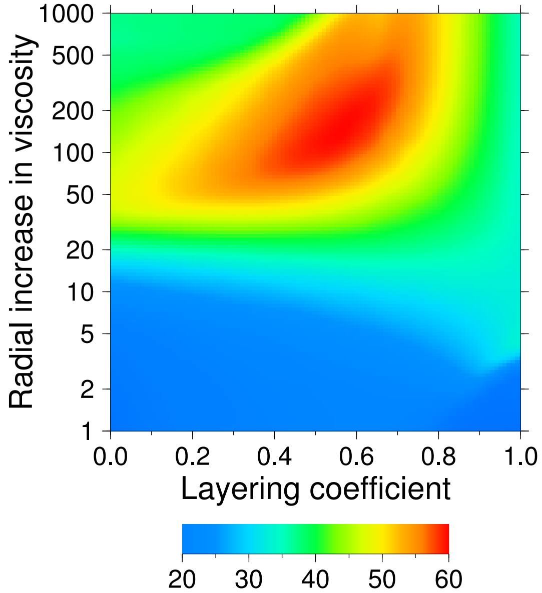

SC+slabs+young oceans

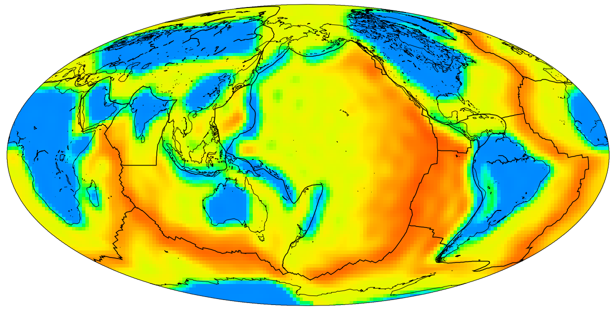

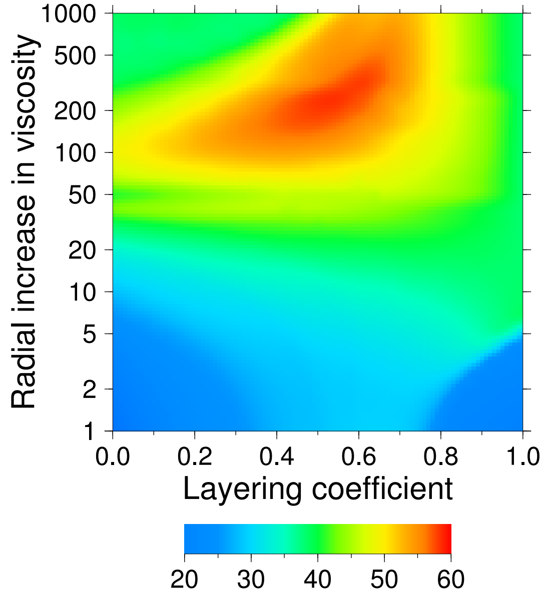

Predicted gravity [%]

LVV: Stable continents (SC)

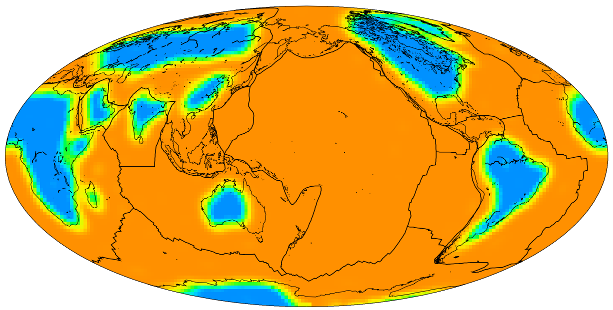

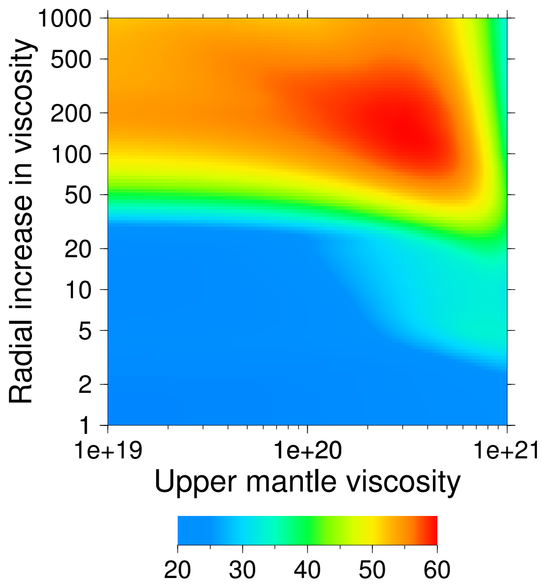

SC+slabs+young oceans

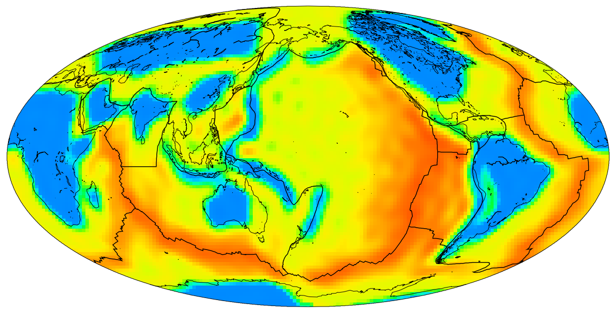

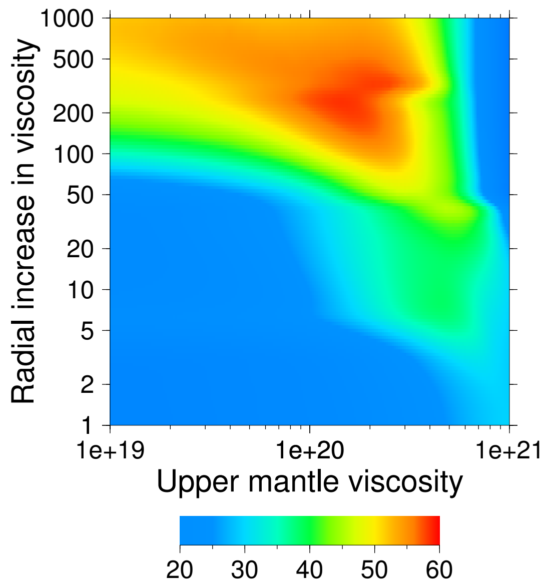

Fitting the geoid and free-air gravity - Summary I

Percentage of predicted data

best-fitting model	free-air gravity	geoid
no LVV whole-mantle flow ($\lambda = 0$)	42%	73%
LVV included whole-mantle flow ($\lambda = 0$)	47%	78%
LVV and partial layering included ($\lambda = 0.6$)	**60%**	**91%**

Impact of LVV

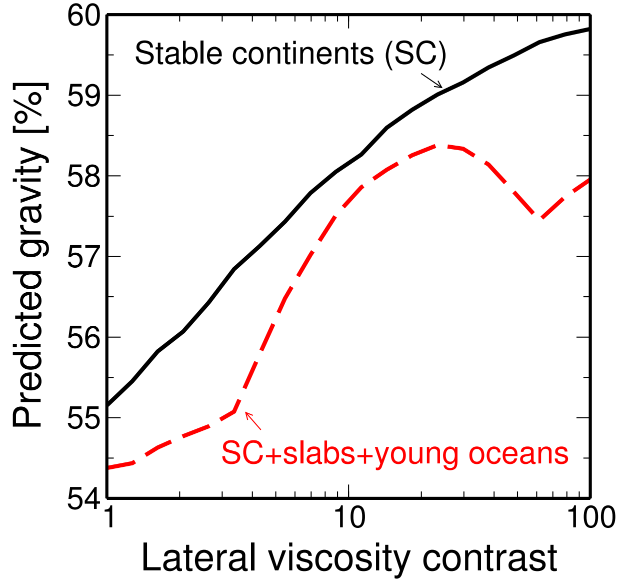

Fitting the geoid and free-air gravity - Summary II

Best-fitting model parameters

	optimum value	acceptable
upper-mantle viscosity	3×10^{20} Pas	$< 7 \times 10^{20}$ Pas
lower-mantle viscosity	4.8×10^{22} Pas	$< 1 \times 10^{23}$ Pas
viscosity in asthenosphere below oceans	3×10^{18} Pas	$\leq 5 \times 10^{19}$ Pas
lateral viscosity contrast	≥ 100	> 10
layering coefficient λ	0.58	$0.40 - 0.75$
velocity-to-density scaling (UM)	0.14	$0.05 - 0.20$
velocity-to-density scaling (LM)	0.24	$0.15 - 0.35$

Fitting the dynamic topography

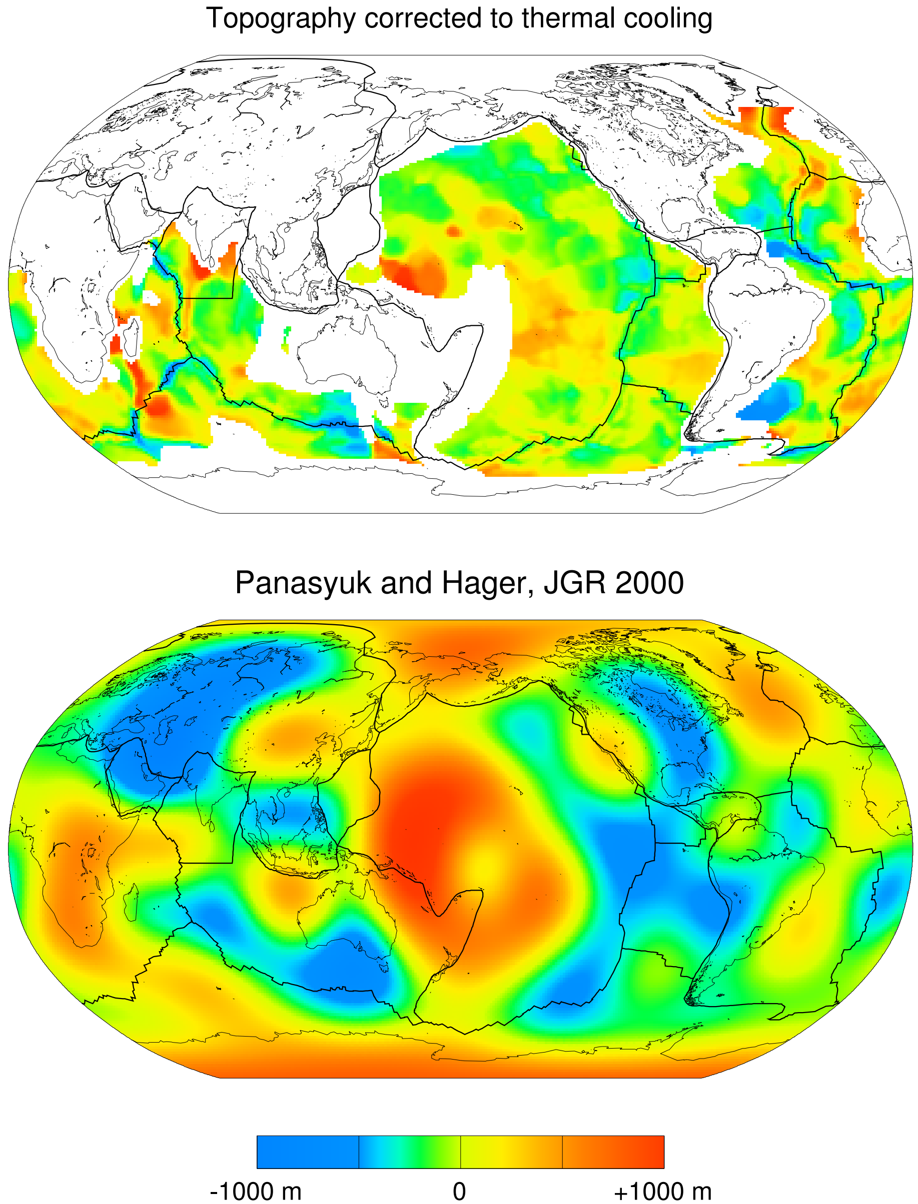

How to formulate the inversion?

- minimuma absolute values
- least-squares
- correlation criterion
- small-amplitude criterion

Data:

- large uncertainties!

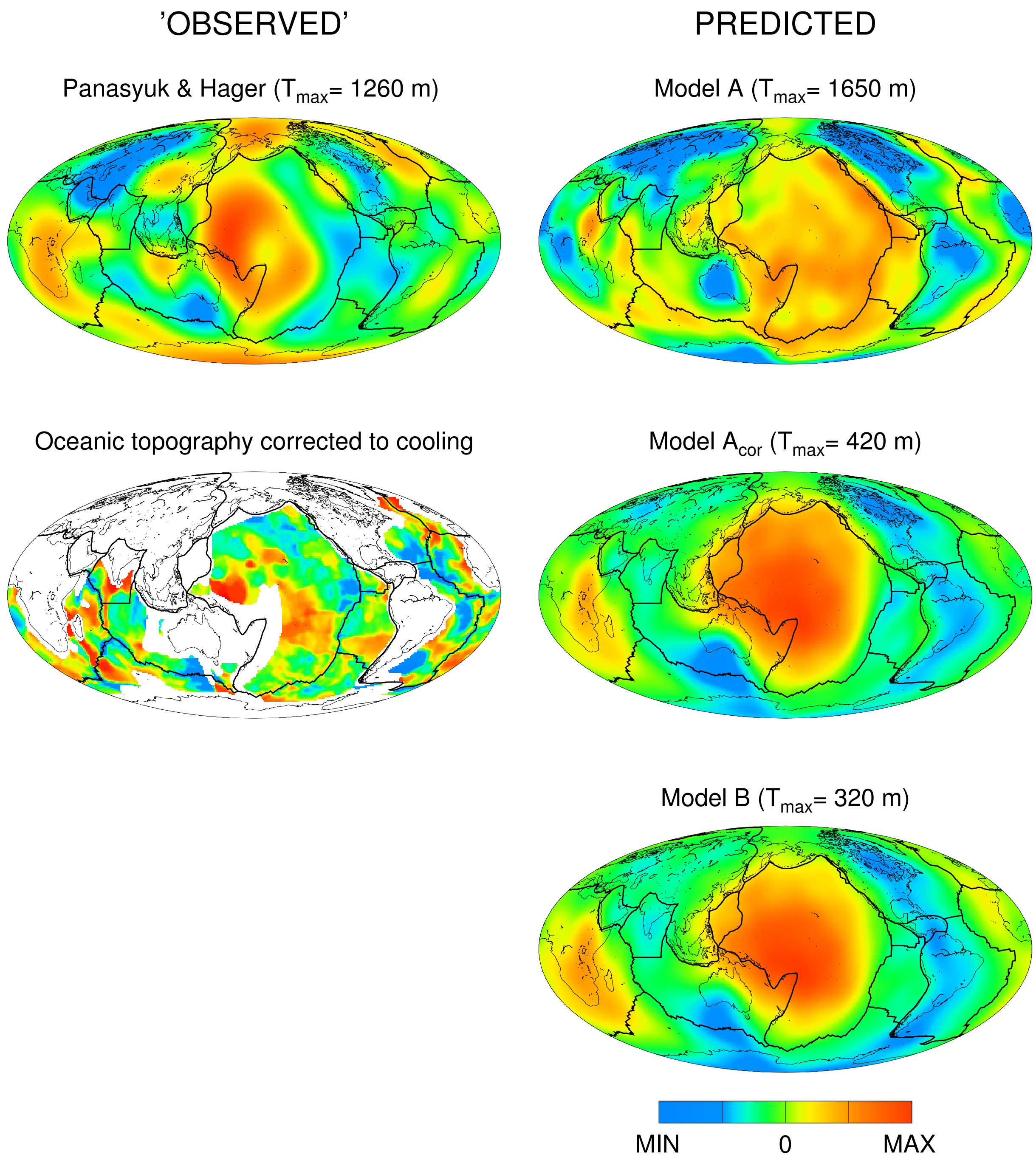

'OBSERVED'
PREDICTED
Panasyuk & Hager (T_{max}= 1260 m)
Model A (T_{max}= 1650 m)
Oceanic topography corrected to cooling
Model A_{cor} (T_{max}= 420 m)
Model B (T_{max}= 320 m)
MIN
0
MAX

Small-amplitude criterion

Model is acceptable if it gives amplitudes smaller than $\sim$ 500 m.
Densities in the top 200 km are omitted.

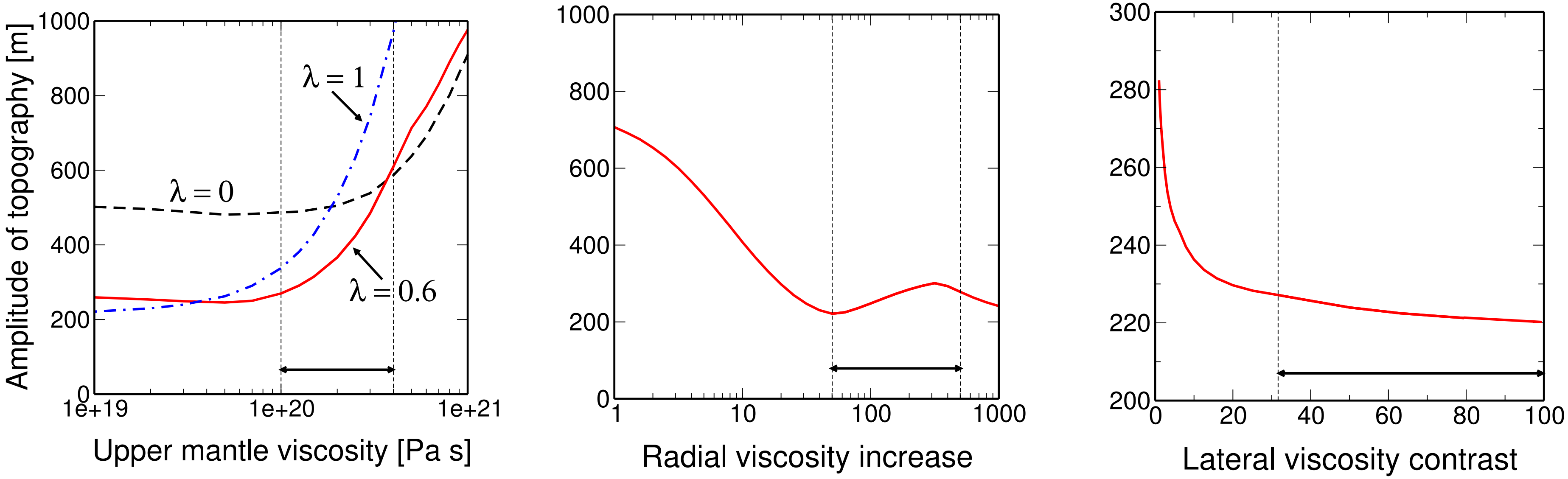

Small-amplitude criterion prefers models with $\lambda \sim 0.6$, $\eta_{UM} \leq 3 \times 10^{20}$ Pa.s and the viscosity increase by a factor of at least 20 in the lower mantle.

Fitting the azimuthal anisotropy

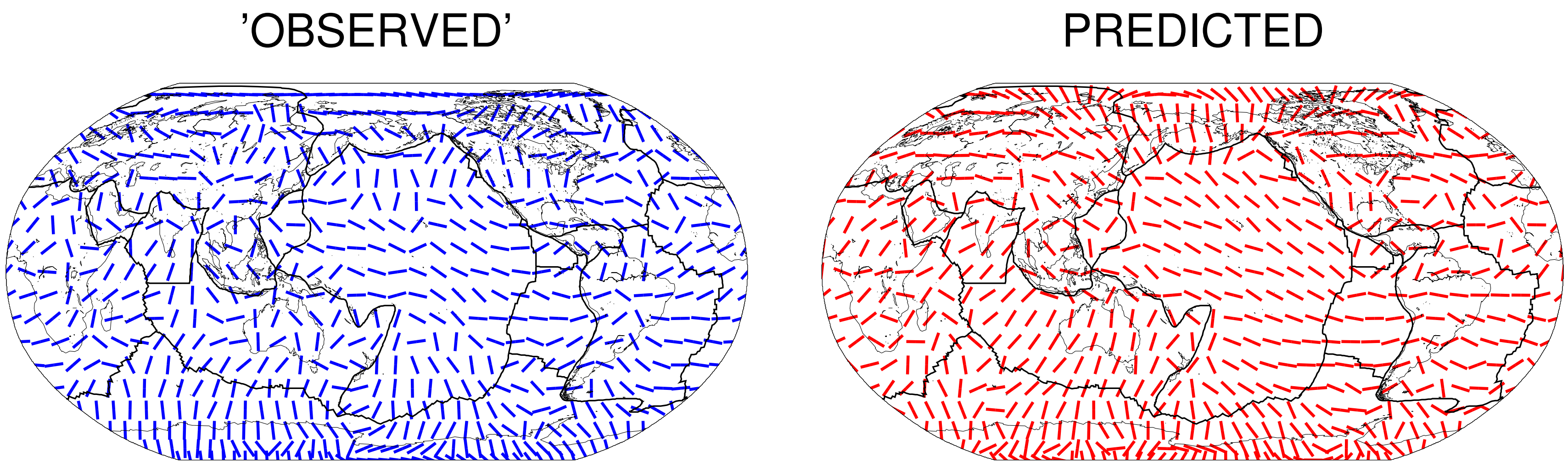

Fitting the azimuthal anisotropy

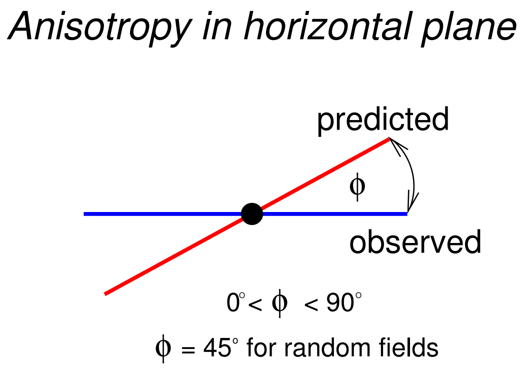

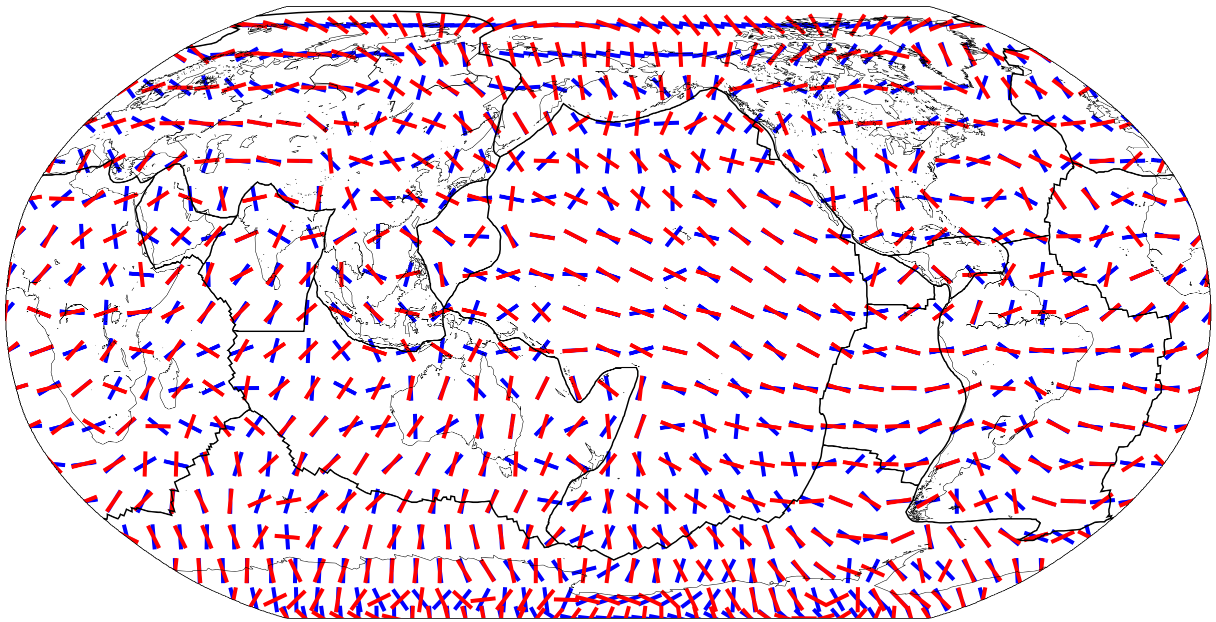

- best agreement with the observation obtained in the depth range of 100-200 km (ϕ=32-35 deg)
- at 300 km, $\phi \sim 40$ degrees
- crutial role of plate motion boundary condition
- solution of inversion is not much influenced by the choice of parameters in DRex code (amount of enstatite, integration time etc.)

Fitting the azimuthal anisotropy - Summary

Resolution of the inverse problem is rather low. Inversion prefers models with a high-viscosity lower mantle. The other parameters, including λ and lateral viscosity contrast, are not resolved.

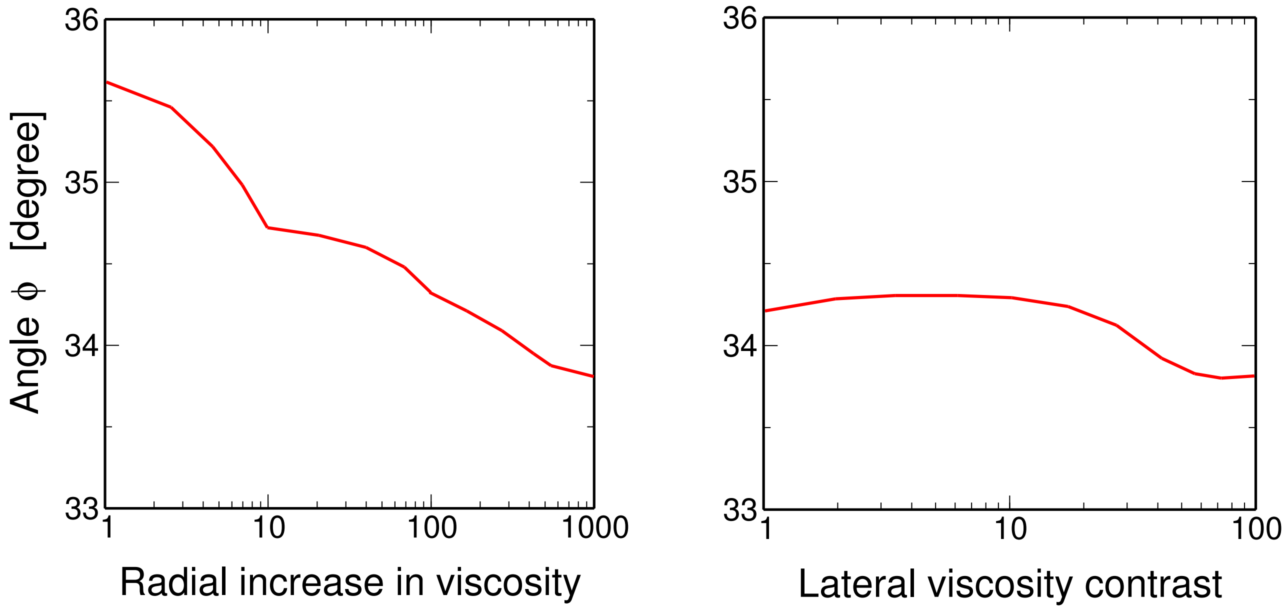

Unsatisfactory fit to the data ($\phi > 32$ deg)! Possible reasons: (i) insufficient knowledge of the density structure in the upper mantle, (ii) linear rheology, (iii) low resolution, (iv) small-scale convection, (v) 'data' errors.

Conclusions

- **Partial layering** ($\lambda \sim 0.6$) is necessary for predicting correct geoid and free-air gravity data if the observed plate motion is prescribed as a BC and small amplitudes of the dynamic topography are requested.
- **Strong lateral viscosity variations** in the top 200-300 km of the mantle, associated with continental roots beneath stable continental regions, further improve the fit to the geoid. The existence of these lateral viscosity variations is neither excluded, nor confirmed by the other data considered.
- Both topographic and seismic anisotropy data prefer models with a **viscosity increase with depth**.
- The correct prediction of **dynamic topography** and **seismic anisotropy** data will require more accurate information on the density structure of the upper mantle.
- Potential of seismic anisotropy data has not yet been fully explored. So far, their inclusion into the inverse modeling has not lead to any significant inprovement of the models.